Article

In Situ NMR Spectroscopy of Combustion

Satyanarayana Anala, Galina E. Pavlovskaya, Prakash Pichumani, Todd J. Dieken, Michael D. Olsen, and Thomas Meersmann

J. Am. Chem. Soc., **2003**, 125 (43), 13298-13302• DOI: 10.1021/ja035838b • Publication Date (Web): 07 October 2003

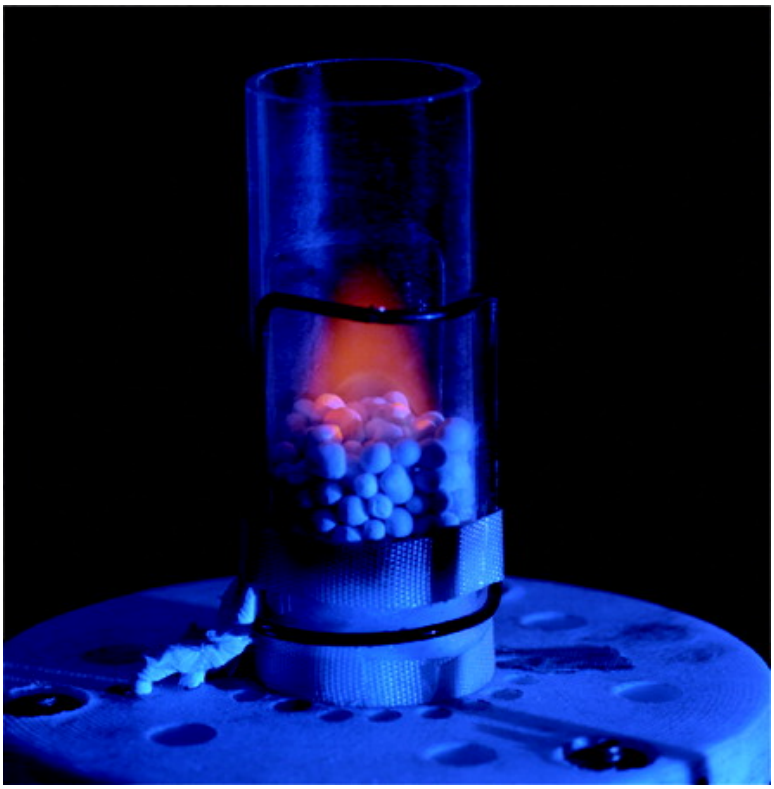

J|A|C|S
ARTICLES
Published on Web 10/07/2003

In Situ NMR Spectroscopy of Combustion

Satyanarayana Anala, Galina E. Pavlovskaya, Prakash Pichumani, Todd J. Dieken, Michael D. Olsen, and Thomas Meersmann*

Contribution from the Department of Chemistry, Colorado State University, Fort Collins, Colorado 80523

Received April 28, 2003; E-mail: meer@lamar.colostate.edu

Abstract: The first successful in situ studies of free combustion processes by one- and two-dimensional NMR spectroscopy are reported, and the feasibility of this concept is demonstrated. In this proof-of-principle work, methane combustion over a nanoporous material is investigated using hyperpolarized (hp)-xenon-129 NMR spectroscopy. Different inhomogeneous regions within the combustion cell are identified by the xenon chemical shift, and the gas exchange between these regions during combustion is revealed by two-dimensional exchange spectra (EXSY). The development of NMR spectroscopy as an analytical tool for combustion processes is of potential importance for catalyzed reactions within opaque media that are difficult to investigate by other techniques.

Introduction

In situ nuclear magnetic resonance spectroscopy (NMR) of high-temperature reactions is of potential value for the investigation of catalytic combustion and other high-temperature applications of catalysts such as partial oxidation of hydrocarbons and steam reforming. Unlike open flames where reactions take place within an optically transparent region, the reaction zone in catalytic processes is located within an opaque medium. Noninvasive measurements of gas and reaction dynamics within the interior of a combustor are therefore challenging. The radio frequency regime provides a previously unused technology to investigate reaction processes in these optically nontransparent systems. In this publication, in situ NMR of combustion using hyperpolarized (hp)-xenon-129 is demonstrated. Uncatalyzed (i.e., free) methane combustion above a region with nanoporous material (i.e., Na-X zeolite pellets) is used for proof of principle illustrating the prospect of in situ NMR of catalyzed combustion. It is shown how the ^{129}Xe NMR chemical shift can be utilized to identify different regions in high-temperature reactions. Two-dimensional (2D) studies of gas exchange within different heat zones of the combustion process provide valuable insights into the gas-phase dynamics. High signal intensity for ^{129}Xe NMR is obtained using hp-xenon produced by spin-exchange optical pumping.[1−4] Optical pumping leads to an increase of the signal intensity by 4 to 5 orders of magnitude compared to conventional ^{129}Xe NMR and has been successfully applied for material science studies of porous media [5−12] and for flow and diffusion measurements.[12−16] The value of ^{129}Xe NMR using thermally polarized (i.e., nonoptically pumped) xenon for intracrystalline hydrocarbon diffusion studies at low temperature in heterogeneous catalysts has been demonstrated extensively in the recent past.[17−21]

The combustion process within the coil region of the NMR probe head (Figure 1) takes place on and above the surfaces of molecular sieve pellets (i.e., only partially dehydrated Na-X zeolite). Although catalytic activity of this material is not expected, the reaction may still be influenced by the zeolite surface in contact with the flame. The methane is premixed with hp-^{129}Xe outside the probe head and enters the high-field coil region from below through a 2 mm vent located just beneath the zeolite pellets. A continuous stream of air (used as an

(1) Raftery, D.; Long, H.; Meersmann, T.; Grandinetti, P. J.; Reven, L.; Pines, A. *Phys. Rev. Lett.* **1991**, *66*, 584−587.
(2) Seydoux, R.; Pines, A.; Haake, M.; Reimer, J. A. *J. Phys. Chem. B.* **1999**, *103*, 4629−4637.
(3) Walker, T. G.; Happer, W. *Rev. Mod. Phys.* **1997**, *69*, 629−642.
(4) Zook, A. L.; Adhyaru, B. B.; Bowers, C. R. *J. Magn. Reson.* **2002**, *159*, 175−182.
(5) Bonardet, J. L.; Fraissard, J.; Gedeon, A.; Springuel-Huet, M. A. *Catal. Rev.—Sci. Eng.* **1999**, *41*, 115−225.
(6) Moudrakovski, I. L.; Lang, S.; Ratcliffe, C. I.; Simard, B.; Santyr, G.; Ripmeester, J. A. *J. Magn. Reson.* **2000**, *144*, 372−377.
(7) Kaiser, L. G.; Meersmann, T.; Logan, J. W.; Pines, A. *Proc. Natl. Acad. Sci. U.S.A.* **2000**, *97*, 2414−2418.
(8) Kneller, J. M.; Soto, R. J.; Surber, S. E.; Colomer, J. F.; Fonseca, A.; Nagy, J. B.; Pietrass, T. *J. Magn. Reson.* **2000**, *147*, 261−265.
(9) Nossov, A. V.; Soldatov, D. V.; Ripmeester, J. A. *J. Am. Chem. Soc.* **2001**, *123*, 3563−3568.
(10) Terskikh, V. V.; Moudrakovski, I. L.; Breeze, S. R.; Lang, S.; Ratcliffe, C. I.; Ripmeester, J. A.; Sayari, A. *Langmuir* **2002**, *18*, 5653−5656.
(11) Moudrakovski, I. L.; Terskikh, V. V.; Ratcliffe, C. I.; Ripmeester, J. A.; Wang, L. Q.; Shin, Y. S.; Exarhos, G. J. *J. Phys. Chem. B.* **2002**, *106*, 5938−5946.
(12) Goodson, B. M. *J. Magn. Reson.* **2002**, *155*, 157−216.
(13) Mair, R. W.; Wong, G. P.; Hoffmann, D.; Hurlimann, M. D.; Patz, S.; Schwartz, L. M.; Walsworth, R. L. *Phys. Rev. Lett.* **1999**, *83*, 3324−3327.
(14) Brunner, E.; Haake, M.; Kaiser, L.; Pines, A.; Reimer, J. A. *J. Magn. Reson.* **1999**, *138*, 155−159.
(15) Meersmann, T.; Logan, J. W.; Simonutti, R.; Caldarelli, S.; Comotti, A.; Sozzani, P.; Kaiser, L. G.; Pines, A. *J. Phys. Chem. A.* **2000**, *104*, 11665−11670.
(16) Kaiser, L. G.; Logan, J. W.; Meersmann, T.; Pines, A. *J. Magn. Reson.* **2001**, *149*, 144−148.
(17) SpringuelHuet, M. A.; Nosov, A.; Karger, J.; Fraissard, J. *J. Phys. Chem.* **1996**, *100*, 7200−7203.
(18) Magalhaes, F. D.; Laurence, R. L.; Conner, W. C.; SpringuelHuet, M. A.; Nosov, A.; Fraissard, J. *J. Phys. Chem. B.* **1997**, *101*, 2277−2284.
(19) Bonardet, J. L.; Domeniconi, T.; N'Gokoli-Kekele, P.; Springuel-Huet, M. A.; Fraissard, J. *Langmuir* **1999**, *15*, 5836−5840.
(20) N′Gokoli-Kekele, P.; Springuel-Huet, M. A.; Fraissard, J. *Adsorption* **2002**, *8*, 35−44.
(21) N'Gokoli-Kekele, P.; Springuel-Huet, M. A.; Bonardet, J. L.; Dereppe, J. M.; Fraissard, J. *Bull. Pol. Acad. Sci., Chem.* **2002**, *50*, 249−258.

10.1021/ja035838b CCC: $25.00

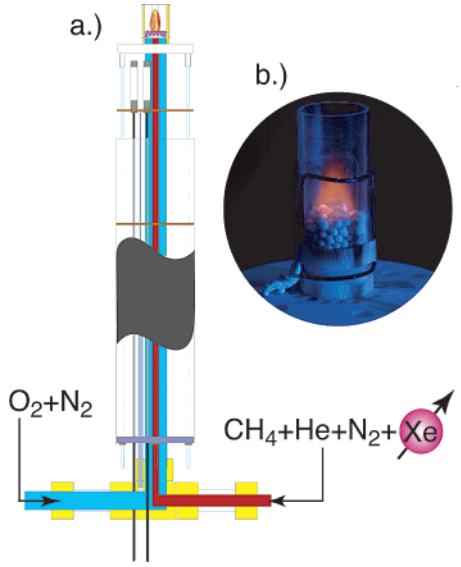

Figure 1. (a) Sketch of the probe head for the in situ study of combustion by hp-^{129}Xe NMR spectroscopy. The hp-xenon is premixed with the methane before both gases enter the probe head. Air as an oxidant is added immediately before the combustion area. (b) A photograph of the NMR coil region during methane combustion. The upper surface of the Na−X zeolite pellets may participate as a catalyst in the reaction. A 39% methane/3% hp-xenon/53% helium/5% nitrogen mixture and air are introduced through two separate outlets and partially mixed within the pellet region. A series of air outlets surrounds the coil region for cooling purposes.

oxidant) enters the detection cell through multiple outlets surrounding the methane−xenon vent. Partial mixing of the gases takes place between the pellets before the educts reach the combustion zone at the upper end of the pellet region. Special care is taken to air cool the NMR probe and the bore of the superconducting magnet without disturbing the combustion process. Figure 2 provides an overview of the experimental setup.

Results and Discussion

1D NMR Spectra. One-dimensional hp-xenon-129 NMR spectra of the gas mixture flowing through the detection region during combustion (red solid lines) and without combustion (blue dashed lines) are shown in Figure 3a. A 700 kPa helium gas mixture containing 5% xenon (and 8% N_2) was used for optical pumping and continuously mixed with methane gas at ambient pressure resulting into approximately 3% xenon, 53% helium, and 40% methane. The ^{129}Xe NMR signal of the gas phase above the porous material without combustion was utilized as the 0 ppm reference standard. During combustion, the ^{129}Xe NMR signal from the reaction zone above the zeolite pellets is shifted upfield by about 29 Hz to −0.26 ppm (Figure 3b). Without the porous material, a nearly identical xenon upfield shift (i.e., 33 Hz) during methane combustion is recorded and depicted in Figure 4. Among the factors that may contribute to this upfield shift are the reduced gas density within the high-temperature zone, the change of the gas composition due to the chemical reaction, and the temperature dependence of the first and second virial coefficient of the chemical shift.[22,23] The second virial coefficient is due to binary collisions and therefore temperature dependent. The first viral coefficient of the chemical shift for monatomic gases is typically temperature independent for temperatures usually accessible in NMR spectroscopy unless the electronic structure is affected. This may be the case at the high combustion temperatures, but neither experimental nor theoretical xenon chemical shift data is available in current literature for temperatures above 1000 K.

The appearance of a second gas-phase signal at −3 ppm is only observed during combustion in the presence of the zeolite (Figure 3; see Figure 4 for comparison). It will be demonstrated in the discussion of the 2D data below that the 350 Hz broad signal at −3 ppm originates from a region just above the bulk of the zeolite. Temperatures in this region are likely to be higher than those in the bulk of the flame, either because of some catalytic activity on the zeolite surface or because of an improved premixing with the oxidant. An increased temperature at the interface to the zeolite may cause the upfield shift to −3 ppm. An alternative explanation is that magnetic susceptibility effects in this region may be responsible for this upfield shift. The shoulder in the spectrum in Figure 3 without combustion is most likely caused by susceptibility effects at the interface. During combustion, the gas flow in the region just above the material may be reduced. This would lead to a more pronounced magnetic susceptibility effect and may be responsible for the −3 ppm peak. It will be left to future experiments (such as flow field measurements) to reveal the exact cause of the this peak. However, in either case, its spatial origin is likely to be at the interface between the material and the gas-phase region.

The xenon chemical shift within the porous material is also affected by temperature. At room temperature, the xenon inside the nanoporous zeolite pellets resonates at approximately 72 ppm (Figure 3a). The signal is shifted to about 68 ppm once the mixture is ignited because the temperature of the material in the precombustion region increases through thermal conductivity and IR radiation. In general, the xenon shift within a nano- or microporous material is strongly affected by the temperature-dependent xenon loading.[24,25] Temperature gradients within the porous material may be responsible for the additional signal broadening of 930 Hz compared to 700 Hz without combustion.

2D Exchange Spectra. Xenon transfer between the nanoporous material and the different temperature regions in the flame was investigated by 2D hp-^{129}Xe NMR exchange spectroscopy (EXSY).[26] The absence of cross-peaks (Figure 5a) demonstrates that exchange between the various regions does not occur during short exchange times $\tau \leq 5$ ms. The corresponding 1D spectrum is displayed above the EXSY for clarity. A significant difference between the common usage of EXSY for the study of chemical exchange and the present usage for the visualization of gas dynamics becomes apparent in Figure 5b−d. Usually, identical back and forward exchange rates in equilibrium systems lead to a symmetric appearance of cross-peaks on both sides of the diagonal. In contrast, the asymmetric appearance of cross-peaks in Figure 5 is a clear signature of a directed exchange that is only present in nonequilibrium systems. The combustion process is in a nonequilibrium steady state because the educts are constantly fed into the combustion zone while the exhaust gases continuously leave the reaction region.

(22) Jameson, C. J.; Jameson, A. K.; Kostikin, P.; Baello, B. I. *J. Chem. Phys.* **2000**, *112*, 323−334.
(23) deDios, A. C.; Jameson, C. J. *J. Chem. Phys.* **1997**, *107*, 4253−4270.
(24) Jameson, C. J.; Jameson, A. K.; Gerald, R. E.; Lim, H. M. *J. Phys. Chem. B.* **1997**, *101*, 8418−8437.
(25) Jameson, C. J.; Jameson, A. K.; Cohen, S. M. *J. Chem. Phys.* **1976**, *65*, 3401−3406.
(26) Jeener, J.; Meier, B. H.; Bachmann, P.; Ernst, R. R. *J. Chem. Phys.* **1979**, *71*, 4546−4553.

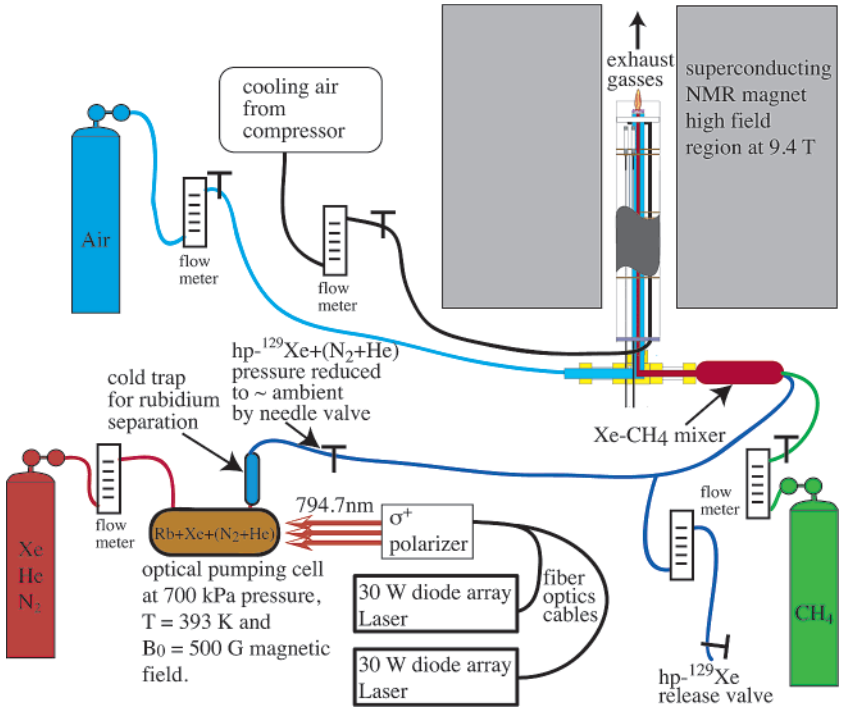

Figure 2. Sketch of the overall set up used for the combustion experiments (see Experimental Section for further details).

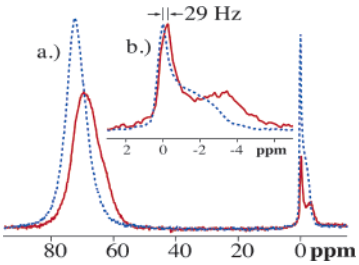

Figure 3. (a) Hp-^{129}Xe NMR spectra at 110.683 MHz of xenon in the combustor using 256 scans, without combustion (blue dashed line) and with ongoing combustion (red solid line). The relative intensities of the two spectra are shown in arbitrary units. (b) An enlargement of the region, 2 ppm $\geq \sigma \geq -4$ ppm, with adjusted intensities that make the 29 $\pm$ 3 Hz gas-phase shift during combustion more apparent. The -3 ppm signal is unique to the combustion process above the nanoporous material.

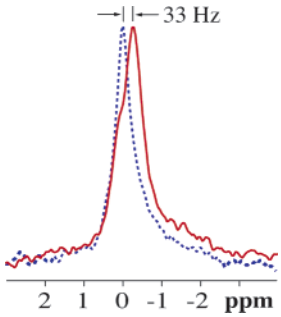

Figure 4. Gas-phase hp-^{129}Xe NMR spectra using 256 scans and the same mixture as in Figure 3 but without the presence of the nanoporous zeolite. The blue dashed line corresponds to the room-temperature gas phase (0 ppm), while the red solid line shows the spectrum during combustion that is the result of a superposition of two signals. One signal arises from the bulk of the gas within the flame area that exhibits a -33 ± 3 Hz shift (-0.27 ppm), and the other signal originates from the gas mixture that is still at room temperature and resonates at around 0 ppm. The latter signal is caused by xenon/methane within the quartz capillary delivery system before mixing with air and entering the combustion region. For clarity, the two spectra are adjusted to equal intensities. The relative intensities are similar to those shown in Figure 3a.

At $\tau = 20$ ms, a cross-peak appears because of the exchange between xenon located in the nanoporous material and the gas phase. A similar peak on the other side of the diagonal is absent since it could only be caused by a reverse exchange against the gas flow direction. Note that xenon gas in the relatively small voids separating the zeolite pellets is neglected for this discussion. Closer inspection of the cross-peak shows that transfer of xenon from the zeolite takes place only to a particular part of the gas phase, namely the region that gives rise to the signal at -3 ppm and not to the one around 0 ppm. Figure 5b also shows a cross-peak that demonstrates exchange from the -3 ppm to the -0.26 ppm region. When the EXSY data in combination with the general direction of the gas flow are taken into account, it can be concluded that the -3 ppm zone is located between the porous material and the bulk of the flame region further above. For longer τ times (see Figure 5c and d), an exchange cross-peak directly between the material phase and the gas phase at 0.27 ppm appears, while the diagonal gas-phase peaks disappear as gas exits the combustion zone (i.e., exchange with regions outside the detection coil).

High Density Optical Pumping. Conventional optical pumping uses approximately 1−5% of xenon in a mixture that contains predominately helium. This allows only for small quantities of xenon to be added to the methane. However, due to the absence of helium in high-xenon-density optical pumping[27] the use of higher xenon concentration in methane is possible. The spectrum in Figure 6 was recorded with approximately 30% xenon in methane without helium. The signal from this mixture for the porous material during combustion (at 67 ppm, red solid line) clearly "tails off" toward the higher ppm region (i.e., downfield). This is indicative of a temperature gradient inside the material that was less visible with a lower concentration of xenon in the gas mixture. The increased

(27) Mortuza, M. G.; Anala, S.; Pavlovskaya, G. E.; Dieken, T. J.; Meersmann, T. *J. Chem. Phys.* **2003**, *118*, 1581−1584.

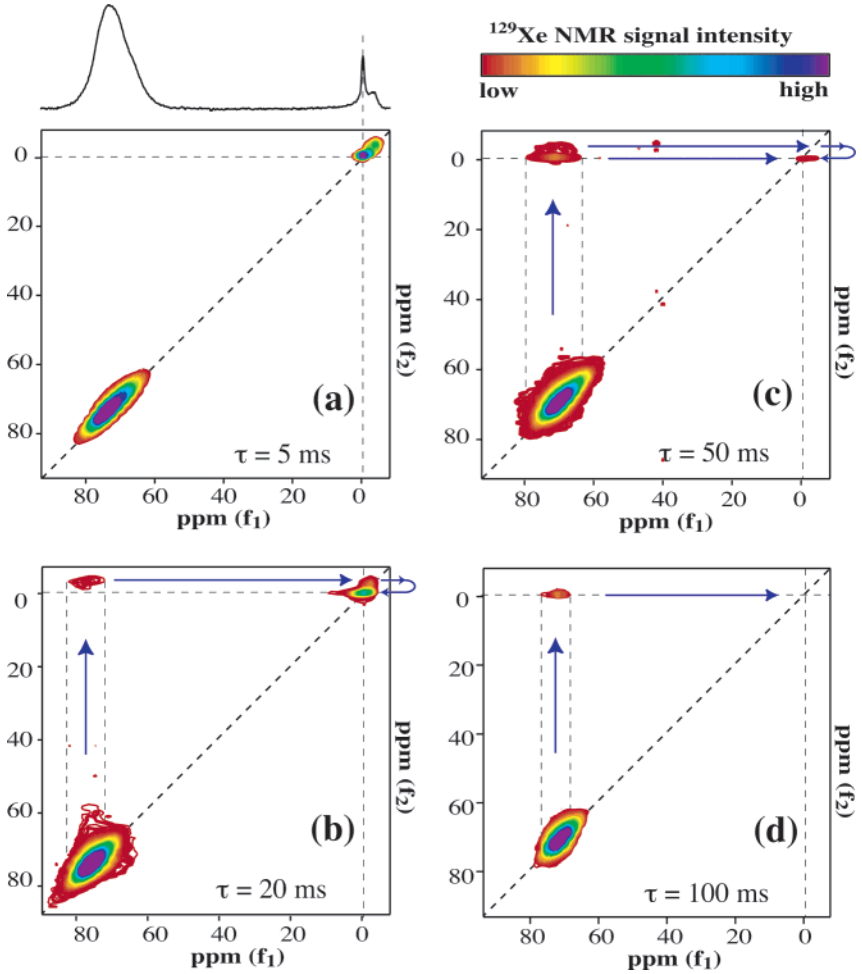

Figure 5. 2D exchange spectra recorded during combustion. The spectra were obtained at 110.683 MHz with 32 × 128 (raw) data points and hypercomplex frequency discrimination (States) with 64 scans per spectrum. The average experimental time per EXSY with a 0.5 s recycle delay was about 40−50 min. (a) No exchange is visible in the EXSY with the exchange time $\tau = 5$ ms. (b−d) With increasing exchange times, cross-peaks appear in an asymmetric fashion while the gas-phase diagonal peaks start to disappear.

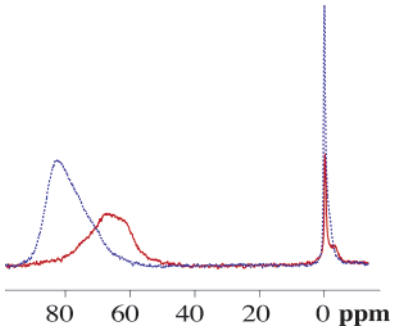

Figure 6. Hp-^{129}Xe NMR spectra with 30% xenon (from high-density xenon optical pumping) in 70% methane. The experimental setting is as described in Figures 1 and 3a. The spectrum in the absence of combustion is shown in a blue dashed line, and the spectrum during combustion, in a red solid line. The relative intensities of the two spectra are shown in arbitrary units.

temperature sensitivity may be attributed to the increased xenon loading in the porous material due to the higher xenon gas concentrations. The increased xenon loading could also amplify the sensitivity of the xenon chemical shift to temperature variations. However, it is also possible that the temperature gradient within the sample has actually been enlarged since the thermal conductivity of the gas phase is reduced without the presence of helium. This could be explored by future high-xenon-density optical pumping experiments where low xenon concentrations in >90% methane would be used without the presence of helium. Most importantly, mixtures with small quantities of xenon as the only optical pumping gas in methane would allow for experiments with very little disturbance of the combustion process. More efficient high-density optical pumping procedures for in situ combustion NMR are currently under exploration.

Conclusion

It is concluded that hp-xenon promises to be a very useful tool for in situ studies of combustion processes that may elucidate heat distribution throughout various regions. Clearly, the quantification or calibration of the temperature dependence of the xenon chemical shift will not be straightforward because of the changing gas composition within a combustion region. The present study shows, however, that even a qualitative interpretation of the chemical shift (or the mere usage in a simple "fingerprint" fashion) can provide essential information about the combustion process.

Extensive experiments and calculations in the recent past have demonstrated the value of ^{129}Xe NMR spectroscopy for investigating intracrystallite diffusion of hydrocarbons in porous catalytic material.[17,18,20] In particular, the combination of ^{129}Xe NMR spectroscopy with ^{1}H magnetic resonance imaging (MRI)

has been proven very insightful.[19,21] These studies have been typically performed in a time-resolved fashion at low temperatures. Much shorter time scales can be expected for high temperature experiments, but similar experiments should still be possible, either because of the use of hp-xenon that requires less signal averaging or because of steady state reaction conditions. Note that a particular spatial coordinate in a steady state system will refer to a particular point in time of the ongoing reaction. Despite the presence of paramagnetic oxygen and radicals, the xenon relaxation times are sufficiently long for gas exchange studies. Directional exchange in this steady state nonequilibrium system results into highly asymmetric EXSY spectra. The scale of the gas dynamics observed in this communication is sufficiently slow to allow for future chemical-shift-selective spatial imaging. Hp-^{129}Xe NMR combined with ^{129}Xe MRI or ^{1}H MRI may be a very promising tool for in situ studies of high-temperature catalytic oxidation processes within opaque media such as platinum or palladium catalysts[28,29] or nanostructured perovskites or hexaaluminates.[30,31]

Experimental Section

A nonrecirculation continuous-flow setup (see Figure 2), is used with two combined 30 W Coherent diode-array lasers emitting at 794.7 nm and with an approximately 2 nm line width. (The system is similar to the ones described for example in refs 2 and 27; however, a noncirculating, open-flow setup like that in ref 15 is used.) For the low-xenon-density experiments, a 5% xenon, 8% nitrogen in 87% helium mixture at 700 kPa pressure is used. Pure xenon gas at the same pressure is chosen for the high-density optical pumping experiments. After pumping and removal of traces of gas-phase rubidium from the pumping mixture by a cold trap, the gas pressure is reduced to slightly above ambient pressure to produce a low flow rate of 40−150 cm^3/min. This allows optimal pumping conditions in our system. The flow rate is measured at high pressure before the pumping process by a flow meter calibrated for nitrogen (using standard equations for conversion) in order to avoid any depolarization of the xenon by parts of the flow meter. A fraction of the optical pumping gas is then released into the atmosphere in order to control the amount of noble gases mixed with the methane. The individual gas ratios for the different experiments are described in the figure captions. A tube containing constrictions and expansions is applied as a gas mixer in order to ensure a homogeneous gas phase that enters the NMR probe head, as shown in Figure 1. Air from a gas tank is fed to the methane mixture just beneath the coil region with the (if present) porous material.

The probe-head region is air cooled by multiple rings of outlets surrounding the coil region (partially shown in Figure 1). The setup is tested outside the magnet with ongoing combustion for prolonged periods of time within a set of spare shim and spin stacks that are identical to the ones inside the bore of the magnet. The air cooling is optimized until the heating of the shim stack is acceptable (approximately 320 K) without causing any change in the visual appearance of the open flame. The hp-^{129}Xe spectra are recorded with a Chemagnetics 400 MHz NMR spectrometer at 110.68 MHz xenon frequency in a 9.4 T wide-bore (89 mm) superconducting magnet after a thermal equilibrium in the probe region is reached (approximately after 0.5 h).

Acknowledgment. This material is based upon work supported by the National Science Foundation Faculty Early Career Development Program under Grant No. CHE-0135082.

JA035838B

(28) Hayes, R. E.; Awdry, S.; Kolaczkowski, S. T. *Can. J. Chem. Eng.* **1999**, *77*, 688−697.
(29) Hayes, R. E.; Kolaczkowski, S. T.; Li, P. K. C.; Awdry, S. *Chem. Eng. Sci.* **2001**, *56*, 4815−4835.
(30) Zarur, A. J.; Ying, J. Y. *Nature* **2000**, *403*, 65−67.
(31) McCarty, J. G. *Nature* **2000**, *403*, 35−36.